Available online at www.sciencedirect.com
ScienceDirect
Trans. Nonferrous Met. Soc. China 30(2020) 1790−1802
Transactions of Nonferrous Metals Society of China
www.tnmsc.cn

# Enhancing mechanical properties and corrosion performance of AA6063 aluminum alloys through constrained groove pressing technique

Ren-jie FAN[1], Shokouh ATTARILAR[2], Mahmoud SHAMSBORHAN[3,4], Mahmoud EBRAHIMI[5], Ceren GÖDE[6], Hatice Varol ÖZKAVAK[7]

1. Department of Mechanical Engineering, Tongling Vocational and Technical College, Tongling 244061, China;
2. School of Metallurgy and Materials Engineering, Iran University of Science and Technology, Tehran, Iran;
3. Department of Engineering, Mahabad Branch, Islamic Azad University, Mahabad, Iran;
4. Department of Mechanical Engineering, University of Zakho, Zakho, Kurdistan Region, Iraq;
5. Department of Mechanical Engineering, Faculty of Engineering, University of Maragheh, Maragheh, Iran;
6. School of Denizli Vocational Technology, Program of Machine, Pamukkale University, Denizli, Turkey;
7. Department of Mechanical and Metal Technology, Technical Sciences Vocational School, Isparta University of Applied Sciences, Isparta, Turkey

Received 4 June 2019; accepted 13 May 2020

**Abstract:** The use of a constrained groove pressing (CGP) method to plastically deform AA6063 aluminum alloy led to the improved surface properties. It was found that hardness magnitude is dramatically improved and its uniformity is considerably decreased after the first pass, while subsequent passes result in better hardness behavior for the processed material. Also, the elongated grains formed in the first pass of the CGP are gradually converted to the equiaxed counterparts by adding pass numbers. Eventually, higher corrosion resistance of the sample by imposing the CGP process is related to the quick formation of passivation film and the change in the morphology of the second phase and precipitates which hinder their electrochemical reactions and decrease the potential localized attack sites.
**Key words:** mechanical properties; corrosion resistance; aluminum alloy; constrained groove pressing technique; grain refinement; hardness distribution homogeneity

## 1 Introduction

Aluminum and its alloys are among the interesting industrial materials due to their specific properties such as low density (approximately 1/3 compared to steel), non-toxicity, high electrical and thermal conductivities as well as suitable corrosion behavior [1]. Aluminum is also one of the most ductile metals in the earth. Hence, a massive variety of products have been made so far including cans, kitchen utensils, subsea structures, airplane parts, etc. In this regard, aluminum alloys from the Al−Mg (5000) and Al−Mg−Si (6000) series have been widely utilized in the marine environment and aerospace applications instead of steel due to the considerable weight savings; however, their mechanical behavior is among the blind spots [1]. Aluminum in its purity condition has been recognized to be resistant to corrosion in most environments due to its protective oxide; but the corrosion behavior could change according to the alloying conditions, environmental parameters, protective actions, etc. For example, it is well demonstrated that aluminum alloy with the magnesium content of 3 to 5 wt.% is susceptible to intergranular corrosion, especially when it is exposed to the corrosive environment [2,3]. For the

**Corresponding author:** Mahmoud EBRAHIMI; Tel: +98-914-4017268; E-mail: ebrahimi@maragheh.ac.ir
DOI: 10.1016/S1003-6326(20)65339-0

above reasons, it is necessary to introduce a new thermomechanical method in which strength and corrosion properties of the aforementioned alloy would be enhanced.

In the last thirty years, severe plastic deformation (SPD), as one of the successful top−down methods, possesses the capability to grain refinement of materials in the order of ultrafine grains (200−800 nm) or nanostructures (<200 nm) levels [4−7]. It has been clarified that the intensive grain refinement is responsible for the enhancement of tribological, superplastic, and mechanical properties of the processed metals and alloys [8−12]. The grain refinement of materials through various SPD techniques is caused by the increment of dislocations density, the formation of dense dislocations walls (low angle grain boundaries), and transformation of them into the high angle grain boundaries [13−15]. In this regard, various SPD techniques have been designed, manufactured, and investigated. The prominent ones include equal channel angular pressing [16], equal channel forward extrusion [17], friction stir processing [18], high-pressure torsion [19], accumulative roll bonding [20], planar twist extrusion [21], and constrained groove pressing (CGP) [22]. The latter method has been proposed and introduced over the last few years to impose intense plastic strains for the sheet formed samples. During the CGP process shown schematically in Fig. 1, a sample is subjected to orthogonal shear deformation by repetitive pressing under the grooved and flat dies periodically. In the first cycle, the sample is put into a pair of asymmetrically grooved dies and the pressing is done in a way that the gap between the upper and lower dies will be the same as that of the sample thickness. Consequently, pure shear deformation is imposed under the plane-strain condition in the inclined region of the sample. However, the flat region remains undeformed. In the second cycle, the corrugated sample is straightened using the flat die. This straightening under the constrained condition ensures that the previous deformed region is exposed to the reverse shear deformation while the undeformed region remains unchanged. Afterward, the sample is rotated by 180° on the axis normal to the sample's plane. This leads to the deformation of the undeformed region due to the asymmetry of the grooved die. In the third cycle, the flattened sample is corrugated again by means of the asymmetrically grooved die and eventually, in the fourth cycle, the corrugated sample is flattened again by the flat die. These consecutive pressing processes with a pair of grooved and a pair of flat dies cause a uniform effective plastic strain throughout the sample. It should be noted that these four cycles are considered as one pass. Since the thickness and shape of the sheet remain unchanged during the process, repetitive pressing processes of the sample are possible to achieve a material with the desired level of plastic strains. Additionally, sample rotation between consecutive passes of the multi-pass CGP process is essential to invoke different slip systems.

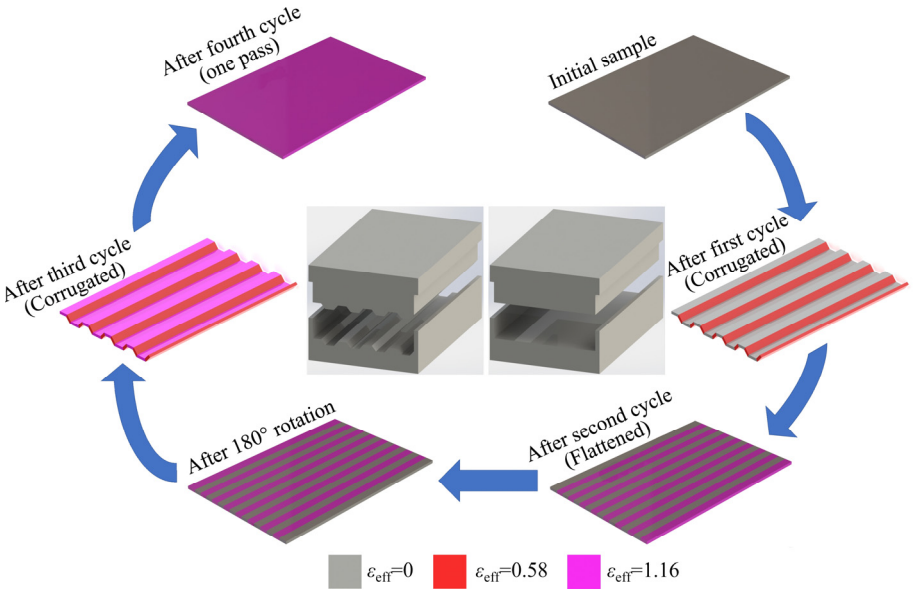


**Fig. 1** Schematic representation of constrained groove pressing (CGP) procedure by means of grooved and flat dies and magnitudes of plastic strain during each cycle

So far, the application of CGP method for processing different metals and alloys and investigating various properties of the deformed samples such as monotonic and dynamic mechanical strength, wear, and superplasticity have been widely carried out [23−25]. JANDAGHI and POURALIAKBAR [26] studied Al−Mn−Si alloy sheets which were severe plastically deformed through CGP up to two passes. The ultimate tensile strength of 196 MPa was obtained which was altered by 54% as compared to the initial condition. Also, elongation to failure of 34% and toughness of 33 J/m$^3$ were achieved for the deformed sample during the post annealing temperature of 350 °C. Investigation of KHODABAKHSHI et al [27] on the mechanical properties of different materials before and after the CGP process showed that common relationships of $\sigma_{YS}/Hv=3$ and $\sigma_{UTS}/Hv=3.45$ ($H_V$ is the Vickers microhardness, $\sigma_{YS}$ and $\sigma_{UTS}$ are the yield strength and ultimate tensile strength, respectively) for coarse-grained (CG) materials are not necessarily applicable for prediction of the hardness−strength relationship in the fine grained and ultrafine grained (UFG) materials. SATHEESH and RAGHU [28] performed the application of CGP process on high purity aluminum sheets up to 5 passes. It was found the subgrain/cell size of 1317 nm after the first pass tends to continuously decrease to 935 nm after the fifth pass. SARKARI KHORRAMI et al [29] studied microstructural and mechanical properties of commercial pure aluminum processed hierarchically by CGP and FSP methods. Although all regions of heat affected zone (HAZ), thermomechanical affected zone (TMAZ), and stir zone (SZ) of CGPed aluminum are quite unstable upon imposing both processes, annealing operation leads to the recrystallization and grain growth in the HAZ and TMAZ. EBRAHIMI et al [30] surveyed tribological behavior of UFG brass samples fabricated by CGP technique and concluded that wear mechanism is transferred from adhesion, delamination, abrasion, and oxidation for the initial condition to the abrasion and adhesion for the third pass processed specimen. Also, a reverse relationship was shown between the specific wear rate and hardness.

According to the above literature review, it seems that corrosion behavior of the CGPed materials has been rarely studied though this property is of significant interest due to the practical importance for industrial utilization. The corrosion resistance of Al−SiC nanocomposite fabricated by accumulative roll bonding was studied by DARMIANI et al [31]. It was noted that imposing the ARB process and the increase of the processing cycles lead to the reduction of pits number due to the uniform distribution of SiC in the aluminum matrix and its refinement. According to the investigation of NIE et al [32], it was observed that the corrosion resistance of commercial pure titanium after being processed by high-pressure torsion (HPT) is lower than that of the initial coarse-grained counterparts; however, the corrosion susceptibility of the HPT-processed titanium decreases with adding torsional strains. This is related to the contradictory connection between the negative effect of the inhomogeneous micro-structure and the positive effect of the grain refinement. NEJADSEYFI et al [33] surveyed the corrosion behavior of 6061 aluminum alloy processed by the combination of heat treatment and ECAP process. The results explained that there are corroded regions selectively in the initial CG sample, leading to the formation of deep and large pits on the sample surface while the shallow and homogeneous corroded surface is achieved after the process. Microstructure evolution effect of ECAPed 304 stainless steel on the corrosion behavior was examined by ZHENG et al [34]. The enhanced corrosion resistance of the deformed sample as compared to the as-received condition is associated with the compactness and stability improvement of the passive film and does not result from the change of its thickness or composition. JIANG et al [35] demonstrated that the increased corrosion resistance of the ECAPed Al−26wt.%Si alloy is attributed to the uniform UFG structure with the breakage of brittle large primary silicon crystals which contribute to a higher pitting resistance. The corrosion behavior of the ECAPed Al−5.4wt.%Ni and Al−5wt.%Cu alloys was examined by AKIYAMA et al [36]. The corrosion resistance improvement of Al−Ni alloy after the ECAP process is dependent on the refining $\alpha$(Al) crystals where pit initiation and growth occur preferentially. Also, the corrosion resistance enhancement of Al−Cu alloy is related to the reduction of the weak points from the Al−Cu alloy in which the Cu-depleted zone surrounding $\theta$ phase precipitates. The corrosion investigation of 6082 aluminum alloy

provided by ECAP technique showed that the higher resistance of pitting corrosion is achieved in comparison with the initial sample [37]. The effect of grain refinement on corrosion behavior of ECAPed pure Mg showed that lower corrosion resistance of the processed sample is strictly associated with the strain-induced crystalline defects including energetic grain boundaries (subgrains) and dislocations [38]. It was found that adding ECAP pass numbers on hypereutectic Al−23%Si alloy makes the voids evanesce and result in the homogeneous UFG structure, leading to a higher pitting resistance [39]. Consequently, enough ECAP pass numbers are useful to improve the corrosion resistance of the aforementioned material. The corrosion behavior of UFG pure aluminum produced by ECAP showed that the improved pitting resistance is achieved from the further stable passive film due to more grain boundaries, larger fraction of non-equilibrium grain boundaries, and residual stress [40]. So, the object of the present communication is to elucidate the effect of CGP processing of AA6063 aluminum alloy on the corrosion behavior and its potential for enhancement of corrosion resistance.

## 2 Experimental

AA6063 aluminum alloy in the form of the plate with the chemical composition of Al−0.57Mg−0.46Si−0.18Fe−0.02Mn−0.02Cu (in wt.%) was used in this study. All samples were cut and prepared with dimensions of 50 mm × 50 mm × 2 mm and subsequently, fully-annealed at 420 °C for 5 h which were cooled slowly at the furnace before the processing. CGP test was performed on the samples up to four passes at ambient temperature using an 80 T oil hydraulic press. Since the width and depth of the corrugated CGP die are equal, each pass number (four successive cycles) imposes the effective plastic strain ($\varepsilon_{\text{eff}}$) of about 1.16 according to Eqs. (1) and (2) [30]. Additionally, Fig. 2 represents the used grooved and flat dies of the CGP process. It was shown by PENG et al [41] that the orientation of sheet specimens by 90° between each consecutive pass number results in the change of deformation plane, and thereby enhanced grain refinement efficiency is achieved compared to the conventional CGP rotation explained above. Also, the maximum strain that can be imparted may be enhanced by changing the orientation of sheets owing to the elimination of repetitive localized deformation. Accordingly, the cross-CGP technique was chosen for this study.

$$y=h/w=1 \tag{1}$$

$$\varepsilon_{\text{eff}}=\left(\frac{4}{3}(y/2)^2\right)^{1/2}=0.58 \tag{2}$$

where $y$, $h$ and $w$ are shear strain, groove height, and groove width, respectively. For this study, the height and width of the grooves are equal.

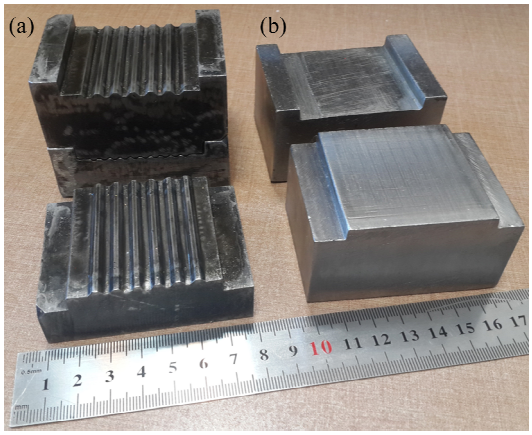


**Fig. 2** Constrained groove pressing operation by means of a pair of asymmetrically grooved dies (a) and a pair of flat dies (b)

Following the CGP, a small square disk with the size of 35 mm near the center of the plate was cut. Afterward, it was mounted and subsequently ground by SiC papers up to 4000 grit and then mechanically polished for hardness measurement and corrosion behavior. Vickers microhardness ($H_{\text{V}}$) measurements were performed on the initial and processed specimens up to the four passes in accordance with the ASTM E384. It is worth mentioning that load and dwell time of Vickers microhardness test were 3 N and 20 s, respectively. Vickers microhardness measurements were carried out over the total surface of each disk following a rectilinear grid-pattern with an interval of 0.5 mm between each separate indentation. The distance of the indentation points was sufficiently spaced to guarantee that the strain hardened regions of measured points do not affect one another. These records were utilized for producing color-coded contour map to show a direct visual representation of the hardness variations across each disk for different CGP pass numbers.

Microstructural examinations were performed using a HITACHI SU−70 field emission scanning electron microscope (FE-SEM) equipped with electron back-scattered diffraction (EBSD) attachment operated at an accelerating voltage of 15 kV. The specimens for EBSD investigation were prepared by manually polishing down to 1 μm diamond polishing followed by mechano-chemically polishing with a 0.05 μm colloidal silica solution using a BUEHLER vibrometer for 24 h. The step sizes of 500 and 50 nm were respectively used for EBSD scanning of the initial and MDF-processed specimens. Eventually, the EBSD data were analyzed by HKL CHANNEL5 software from Oxford instrument.

The prepared disk specimens were rinsed with de-ionized water, degreased by ethanol, and ultrasonically-cleaned with acetone at 40 °C for 15 min to eliminate any residual oxide layer and debris from the CGP operation. After that, electrical contact was performed by connecting a copper wire and then, it was embedded in an epoxy cold resin mounting. The electrochemical experiments were conducted in isotonic aqueous 0.9% NaCl solution (normal saline). The solution was provided with distilled water and reagent grade chemicals. To examine the electrochemical behavior of initial and deformed specimens, conventional three-electrode setup was utilized with the working electrode, saturated standard calomel reference electrode (SCE), and a platinum counter electrode connected to potentiostat/galvanostat (model BHP2063) with the computer-assisted system. The corrosion measurements were conducted at 20 °C. The range of potential scan was from −0.8 to 0.2 V and the open-circuit potential with a scan rate of 1 mV/s was employed for the potentiodynamic polarization. Prior to the immersion of specimens in the test solution, they were put in the solution for 1 h to attain the open-circuit potential. All electrochemical experiments were repeated at least three times in order to obtain the reproducibility of the results. The electrochemical parameters were calculated according to well-known Tafel extrapolation method [42]. Furthermore, to study the corrosion behavior and morphologies, the specimens were mechanically polished in the same manner; then, they were immersed in 4% $H_2SO_4$ aqueous solution at room temperature for 7 d. The samples were examined by scanning electron microscopy (SEM), model TESCAN VEGA with voltage of 20 kV. Also, in order to obtain a localized chemical analysis from the inside and outside of the pores, energy-dispersive X-ray spectroscopy (EDX) measurement was conducted.

## 3 Results and discussion

The variation of microhardness distribution for the AA6063 aluminum sheets before and after the CGP process up to four passes is displayed in Fig. 3. In this regard, standard deviation has been

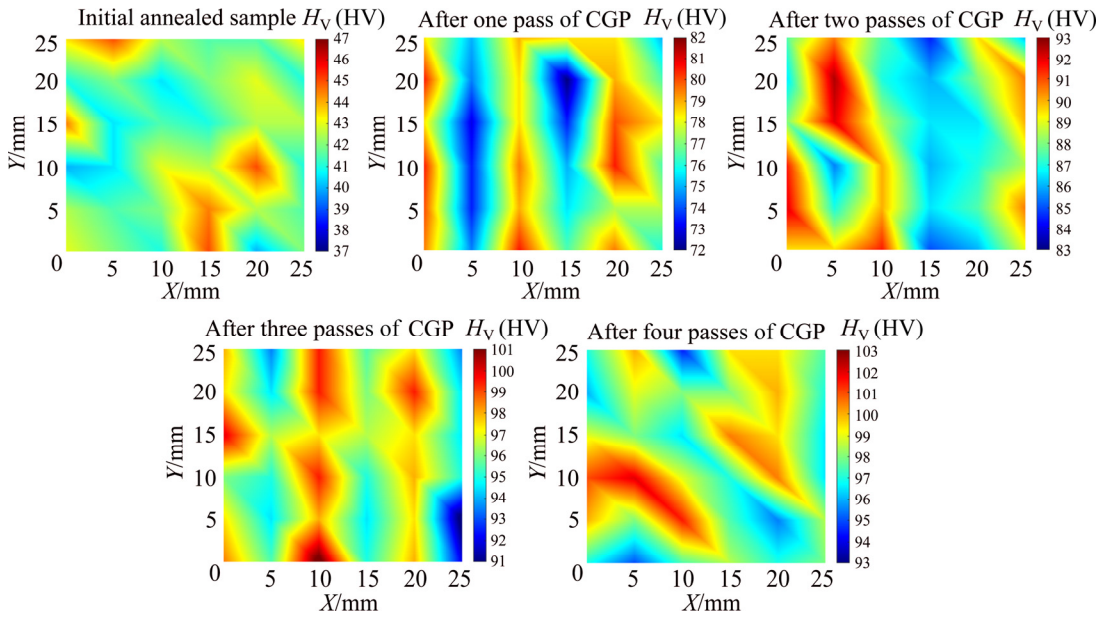


**Fig. 3** Vickers microhardness distribution of AA6063 aluminum alloy before processing and after CGP process up to four passes

utilized in order to quantitatively compare the hardness distribution uniformity. As known, it is a statistical tool to quantify the amount of data variation. Accordingly, a low magnitude for standard deviation means that the data points tend to be close to the average, while a high standard deviation relates to the data points which are spread out over a wider range. Equation (3) represents the aforementioned relationship for measuring the hardness distribution in which SD is the standard deviation, $Hv_1$, $Hv_2$, $Hv_3$, ⋯, $Hv_N$ are associated with the measured magnitudes of each hardness point, $Hv_m$ is the mean magnitude of these measurements, and $N$ is the number of measurements in the sample [43].

$$\mathrm{SD}=\sqrt{\frac{1}{N-1}\sum_{i=1}^{N}(H_{V_i}-H_{V_m})^2} \tag{3}$$

According to Fig. 3 and Table 1, it is found that the initial aluminum sample has the hardness of HV 42.2 with the high-level hardness distribution homogeneity of 1.395. Imposing one pass CGP process on the aluminum sample leads to the considerable hardness improvement up to the level of HV 77.3, while its homogeneity drops significantly. The results showed that about 78% reduction of the hardness distribution uniformity is attained by application of one pass process as compared to the as-received condition. By applying the second pass of the CGP process, the homogeneity of hardness distribution and the magnitude of average hardness are increased a little. The results of the second pass show that about 14% improvement in the average hardness magnitude and approximate 3.5% enhancement in the hardness dispersal uniformity have been achieved in comparison with the previous counterpart. The reason of improving hardness homogeneity is related to the applied route, i.e., cross-orientation pressing procedure. It also permits a sample to have more pressing cycles and thus higher accumulated plastic strains without introducing any considerable cracks to the sheet metal as compared to the single-orientation (conventional) pressing counterpart. Addition of one extra pass number (third pass) to the sheet sample leads to the hardness magnitude and uniformity of HV 96.5 and 2.378, respectively. Eventually, the fourth pass causes the hardness improvement of only about 2% while it homogenizes hardness distribution to about 24% in comparison with the third pass. According to the achieved results, it can be concluded that the first pass has the most influence on the improvement of hardness magnitude and the subsequent passes increase it gradually. Also, hardness distribution uniformity, which has a great reduction within the first pass, is enhanced gradually up to the final pass number.

**Table 1** Average hardness magnitude ($H_V$) and standard deviation of hardness distribution (SD) of AA6063 aluminum alloy after different pass numbers of CGP in comparison with as-received annealed condition

| Process condition | $H_v$ (HV) | SD |
|---|---|---|
| Annealed | 42.2 | 1.395 |
| Pass 1 | 77.3 | 2.491 |
| Pass 2 | 88.3 | 2.403 |
| Pass 3 | 96.5 | 2.378 |
| Pass 4 | 98.2 | 1.806 |

In order to assess the hardenability behavior of AA6063 aluminum sheets after being subjected to the CGP process, a double-natural logarithmic plot of the measured hardness magnitude versus calculated equivalent plastic strain is represented in Fig. 4. Accordingly, the solid-line of this plot depicts a trend of all data points which expresses in the form of Eq. (4) wherein the square of standard deviations, $R^2$, is 0.9828. This relationship indicates the achieved hardenability exponent of 0.18 showing somewhat strong strain-hardening. The achieved hardenability exponent may originate by

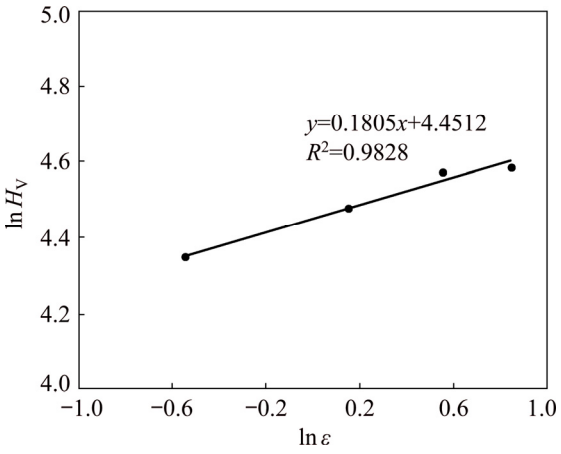


**Fig. 4** Double-natural logarithmic plot of Vickers hardness versus imposed plastic strain for AA6063 aluminum alloy after being subjected to CGP process up to four passes

the comprehensive effects of grain refinement which is associated with the connection between the strength and imposed strain in the deformation processing. The same work has been previously carried out on the high-purity Al, AZ31 alloy, and ZK60A alloy after the HPT process [44−46]. It seems that this approach is an acceptable method for obtaining quantitative information of the hardness evolution in materials processed by SPD method especially CGP technique; however, it needs additional data from various metals and alloys for expanding in the practical applications.

$$H_V=85.7\varepsilon^{0.18} \tag{4}$$

To estimate the strength of processed aluminum based on the measured hardness magnitudes, different studies have been carried out. It has been shown that the UFG materials do not follow the utilized hardness−strength relationships in the conventional coarse-grained counterparts [44,46]. It seems that the most suitable hardness−strength relationship for this aim is related to the work of KHODABAKHSHI et al [27] represented in Eqs. (5) and (6). The modified work-hardening exponent represents the strength of different metals and alloys through various SPD techniques at different pass numbers. Its magnitude is 0.114, 0.122, and 0.152 for the commercial pure aluminum, AA3003 aluminum alloy, and commercial pure copper, respectively [27]. It is worth mentioning that it is calculated by recording the slope of true stress evolution versus equivalent plastic strain through different SPD pass numbers.

$$\mathrm{YS}=\frac{3H_V}{0.1^{-n^*}} \tag{5}$$

$$\mathrm{UTS}=\frac{2.9H_V}{(1-n^*)\left(\frac{12.5n^*}{1-n^*}\right)^{n^*}} \tag{6}$$

where YS and UTS are yield strength and ultimate tensile strength, respectively; $n^*$ is the modified work-hardening exponent.

The improvement of mechanical properties by means of the CGP process may be associated with the microstructure evolution. In this regard, EBSD inverse pole figure (IPF) maps of AA6063 aluminum alloy before and after different passes of CGP process are illustrated in Fig. 5. As can be observed, the microstructure of initial aluminum contains coarse grains with mean grain size of about 100 μm. After one pass of CGP process, some elongated grains with length and width of about 20 and 2 μm respectively are formed in the microstructure. They have an aspect ratio (length/width) of 10:1. Meanwhile, some small equiaxed grains with the sizes less than 2 μm are also presented in this microstructure. The grain colors in the IPF map of one pass CGPed sheet reveal a strong texture which shows the formation

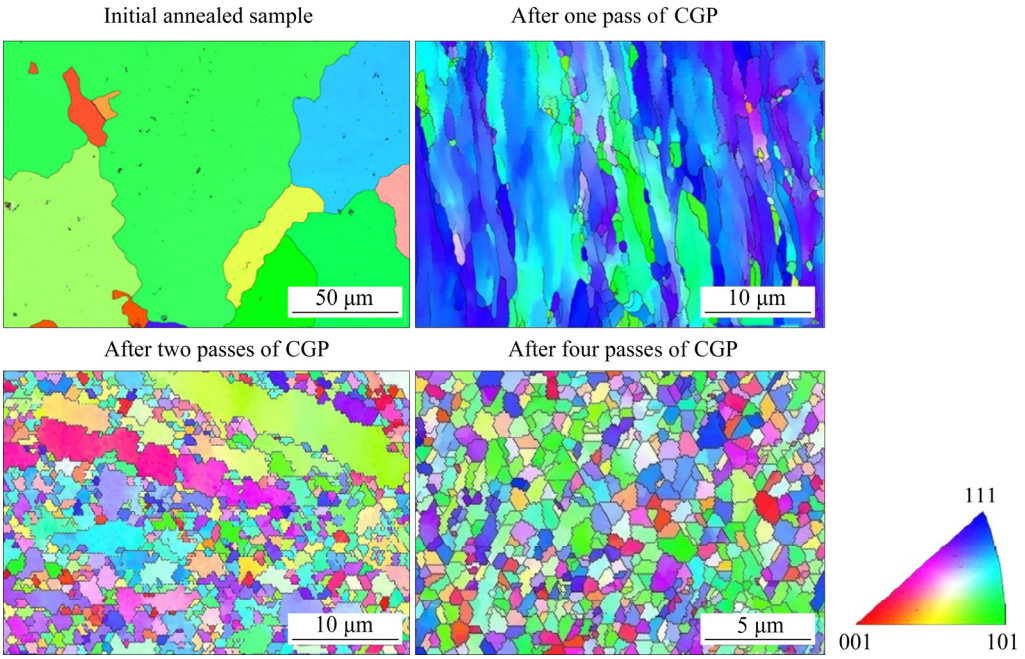


**Fig. 5** EBSD inverse pole figure maps of AA6063 aluminum alloy before and after different CGP processes up to four passes

of preferred orientation. By addition of CGP pass numbers, the elongated grains are converted to the equiaxed counterparts in such a way that the microstructure totally consists of the equiaxed grains in the sample processed by four passes of CGP. The IPF maps of two and four passes CGPed aluminum sheets demonstrate that the strong texture formed after the first pass of process, annihilates within the subsequent passes; therefore, there is no preferred orientation in the fourth pass CGPed sample. It is also obvious after the four passes of CGP process, a homogeneous microstructure with equiaxed grains and average grain size of about 500 nm is formed in AA6063 aluminum alloy. In this regard, the measured hardness behavior is in good agreement with this finding. Similar to other SPD methods, grain segmentation mechanism based on the considerable increment of dislocations density is the main gain refinement mechanism due to the intense shear strains of the CGP process. In this mechanism, grain segmentation occurs by increment of dislocations density and accordingly, low angle grain boundaries (LAGBs) are formed at the initial passes of CGP process. The LAGBs are transformed to high angle grain boundaries (HAGBs) at the subsequent passes and consequently, ultrafine grains with equiaxed shape are formed after the four passes of CGP process [47−50].

The corrosion behavior of AA6063 aluminum alloy through potentiodynamic polarization curves after two and four passes of CGP process in comparison with the initial annealed condition is shown in Fig. 6. It can be easily observed that the overall behavior of all samples is relatively the same while they show different corrosion rates in 0.9% NaCl solution (see Table 2). The electrochemical parameters are also listed in Table 2. Accordingly, the best corrosion behavior of the AA6063 with the least amount of corrosion rate belongs to the fourth pass CGPed sample while the initial annealed sample has the highest corrosion

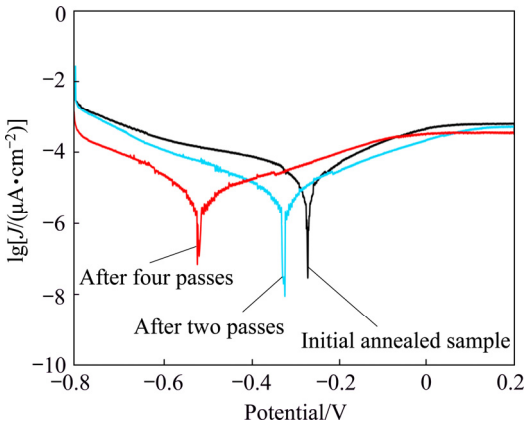


**Fig. 6** Potentiodynamic polarization curves of AA6063 aluminum alloy after different pass numbers of CGP in comparison with as-received annealed sample

rate. Interestingly, the application of CGP process up to the four passes leads to 70.5% reduction of corrosion rate.

It has been known that high purity aluminum due to the alumina passive film formation is highly resistant to corrosion [51]. Previous studies showed some intermetallic precipitates in Al−Mg−Si alloys such as MgSi, $Mg_2Si$, and even AlFeSi [52,53]. These intermetallic precipitates are formed due to the low solubility limit of aluminum matrix [51]. It has also been reported that the intermetallic precipitates play an important role in corrosion behavior of aluminum alloys [54]. Moreover, the morphology, amount, and the distribution of intermetallic precipitates can effectively influence the corrosion performance of the AA6063 aluminum alloy [53]. In addition to intermetallic precipitates, the average grain size and grain boundary propulsion alter the resistance to corrosion, as well [55].

It was found that the application of CGP process leads to a high amount of grain fragmentation, the annealed sample with the average grain size of 100 μm reaches about 500 nm after imposing four passes of the CGP process. SIKORA et al [56] concluded that in Al−Mg based

**Table 2** Electrochemical parameters of AA6063 aluminum alloy after different pass numbers of CGP in comparison with as-received annealed sample

| Sample condition | $R_p$/mV | $J_{corr}$/(μA·cm$^{-2}$) | $B_c$ | $B_a$ | Corrosion rate/(m·a$^{-1}$) |
|---|---|---|---|---|---|
| Initial annealed | 264.95 | 0.151044 | 0.2237 | 0.1564 | 0.0522 |
| Two passes of CGP | 311.23 | 0.118119 | 0.1551 | 0.1859 | 0.0408 |
| Four passes of CGP | 526.36 | 0.04152 | 0.0766 | 0.1412 | 0.01435 |

$R_p$ is polarization potential; $J_{corr}$ is corrosion current density; $B_c$ is cathodic slope and $B_a$ is anodic slope; $a$ is equal to year.

alloys, the grain refinement leads to the reduction of susceptibility to pitting and also, the current densities are lower in the case of nanograined alloy. It is generally reported [56−58] that ultrafine grained Al alloys demonstrate decreased cathodic kinetics, lower current densities, resistance to pitting, improved behavior in mass-loss testing and enhanced resistance to stress corrosion cracking. The reason has been related to easier passivation especially in the NaCl electrolytes which arise from the higher grain boundaries density [40,56]. Another possible reason could result from the alteration in the morphology, distribution, and sizes of the intermetallic precipitates, second phases, and precipitates especially through the physical breakdown of them by severe plastic deformation methods. The breakage of these intermetallic precipitates and second phases is beneficial since it prevents their operation as suitable sites for electrochemical reactions and the initiation of localized attacks [56,58,59]. Hence, it can be claimed that considerable grain size reduction through CGP processing from 100 μm in the initial sample to 500 nm in the fourth pass CGPed sample leads to the higher grain boundaries density and easier formation of alumina passive oxide film. In addition, the grain fragmentation may reduce the sizes of intermetallic precipitates and second phases which hinder their electrochemical reactions and reduce the possible localized attack sites; therefore, the corrosion behavior is improved by increasing the CGP pass numbers. Furthermore, it can be inferred that grain size reduction through CGP application can be a good procedure to enhance the electrochemical and corrosion behavior of Al−Mg−Si alloys in NaCl electrolytes.

Eventually, Fig. 7 shows the SEM micrographs of different samples corroded in 4% $H_2SO_4$ aqueous

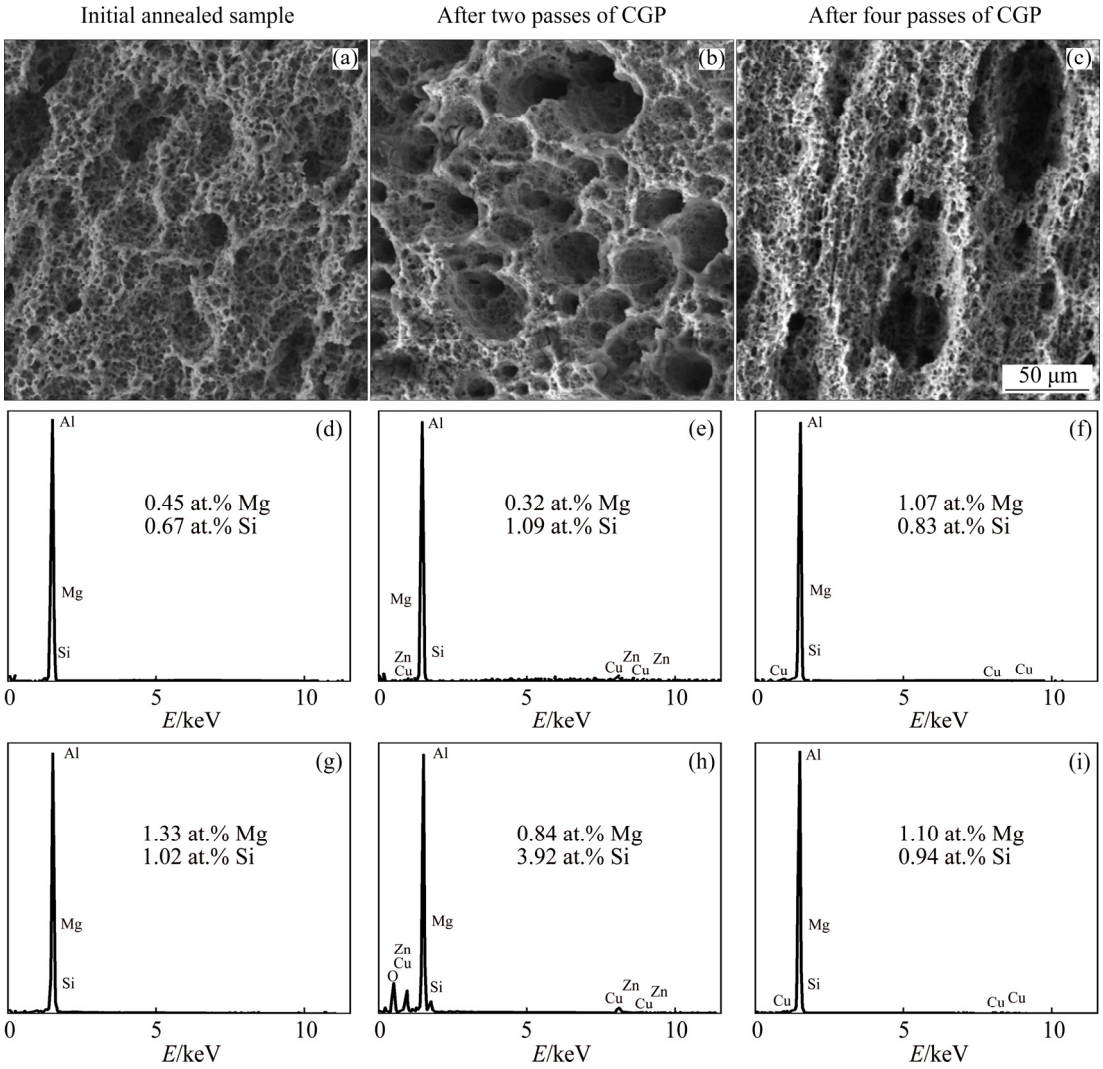


**Fig. 7** SEM images (a−c) and EDX analyses (d−i) of inside (d−f) and outside (g−i) pits of AA6063 aluminum alloy after different pass numbers of CGP in comparison with as-received annealed sample in 4% $H_2SO_4$ aqueous solution for 7 d

solution for 7 d. As it can be observed, the number of the pits is decreased by increasing the pass numbers but they become deep and large. This variation in the morphology and distribution of pits is a direct result of CGP process which alters the distribution and morphology of intermetallic precipitates which finally affect the corrosion behavior. It can be concluded that the decrease of pit numbers due to increasing CGP pass numbers leads to the improvement of the corrosion resistance and possibly the shape and size of pits have lower influence on the corrosion behavior. Also, from the EDX analysis, it can be generally concluded that pits initiate in the regions which are poor of the alloying elements like Mg and Si. Hence, the existence of these elements and the possible MgSi and $Mg_2Si$ intermetallic precipitates are beneficial from corrosion point of view. Thus, the ECAP process and consequently, the grain refinement may alter the morphology and other characteristics of intermetallic precipitates which were previously reported in Ref. [55]; therefore, possibly it also happened in our study and the change of pits morphology is one of the indicators for this phenomenon.

## 4 Conclusions

(1) Lower hardness homogeneity of aluminum sample is attained after imposing one pass and subsequent passes compensate it somewhat. Also, hardness magnitude that increases dramatically after the first pass grows slowly up to the final pass.

(2) By utilization of double-natural logarithmic plot of the measured hardness magnitude versus calculated equivalent plastic strain, the hardenability exponent of CGPed aluminum alloy is obtained to be equal to 0.18 showing somewhat strong strain-hardening.

(3) The increment of dislocations density is the main reason for improving strength mechanism due to the intense shear strains of the CGP process. Also, the effects of grains refinement and presence/ fragmentation of precipitates are considerable.

(4) By the addition of CGP pass numbers, the produced elongated grains within the first pass are gradually transformed to the equiaxed counterparts in such a way that the microstructure totally consists of the equiaxed grains in the order of 500 nm processed by four passes of CGP.

(5) Improving corrosion resistance of AA6063 aluminum alloy by imposing CGP process is related to easier formation of passivation film which arises from the higher grain boundaries density. Also, it may be associated with the alteration in the morphology, distribution, and sizes of the precipitates through physical breakdown of the alloy by CGP technique which hinder their electrochemical reactions and decrease the possible localized attack sites.

(6) The number of pits is decreased by increasing the pass numbers but they become deep and large. Generally, pits imitate in the regions which are poor of the alloying elements; so, the existence of alloying elements and the possible MgSi and $Mg_2Si$ intermetallic precipitates are beneficial from the corrosion point of view.

## Acknowledgments

This work was funded by “Quality Engineering Project of Anhui Province of China in 2016” entitled mold design and manufacturing experimental training center (2016sxzx050).

## References

[1] MUKHOPADHYAY P. Alloy designation, processing, and use of AA6xxx series aluminium alloys [J]. International Scholarly Research Network Metallurgy, 2012: 1−15 (Article ID: 165082).

[2] KUCHARIKOVA L, LIPTAKOVA T, TILLOVA E, KAJANEK D, SCHMIDOVA E. Role of chemical composition in corrosion of aluminum alloys [J]. Metals, 2018, 8: 581−594.

[3] VICERE A, ROVENTI G, PAOLETTI C, CABIBBO M, BELLEZZE T. Corrosion behavior of AA6012 aluminum alloy processed by ECAP and cryogenic treatment [J]. Metals, 2019, 9: 408−421.

[4] VALIEV R Z, LANGDON T G. Principles of equal-channel angular pressing as a processing tool for grain refinement [J]. Progress in Materials Science, 2006, 51: 881−981.

[5] ZHILYAEV A, LANGDON T. Using high-pressure torsion for metal processing: Fundamentals and applications [J]. Progress in Materials Science, 2008, 53: 893−979.

[6] VALIEV R. Nanostructuring of metallic materials by SPD processing for advanced properties [J]. Nature Materials, 2004, 3: 511−516.

[7] DJAVANROODI F, EBRAHIMI M, NAYFEH J F. Tribological and mechanical investigation of multi-directional forged nickel [J]. Scientific Reports, 2019, 9: 1−8.

[8] DJAVANROODI F, EBRAHIMI M, RAJABIFAR B, AKRAMIZADEH S. Fatigue design factors for ECAPed

materials [J]. Materials Science and Engineering A, 2010, 528: 745−750.

[9] LA P Q, MA J Q, ZHU Y T, YANG J, LIU W M, XUE Q J, VALIEV R Z. Dry-sliding tribological properties of ultrafine-grained Ti prepared by severe plastic deformation [J]. Acta Materialia, 2005, 53: 5167−5173.

[10] FARSHIDI M H, KAZEMINEZHAD M, MIYAMOTO H. On the natural aging behavior of aluminum 6061 alloy after severe plastic deformation [J]. Materials Science and Engineering A, 2013, 580: 202−208.

[11] EBRAHIMI M, SHAERI M H, GODE C, ARMOON H, SHAMSBORHAN M. The synergistic effect of dilute alloying and nanostructuring of copper on the improvement of mechanical and tribological response [J]. Composites (Part B): Engineering, 2019, 164: 508−516.

[12] EBRAHIMI M, SHAMSBORHAN M. Monotonic and dynamic mechanical properties of PTCAE aluminum [J]. Journal of Alloys and Compounds, 2017, 705: 28−37.

[13] SABIROV I, BARNETT M R, ESTRIN Y, HODGSON P D. The effect of strain rate on the deformation mechanisms and the strain rate sensitivity of an ultra-fine-grained Al alloy [J]. Scripta Materialia, 2009, 61: 181−184.

[14] HUGHES D A, HANSEN N, BAMMANN D J. Geometrically necessary boundaries, incidental dislocation boundaries and geometrically necessary dislocations [J]. Scripta Materialia, 2003, 48: 147−153.

[15] SAKAI T, BELYAKOV A, KAIBYSHEV R, MIURA H, JONAS J J. Dynamic and post-dynamic recrystallization under hot, cold and severe plastic deformation conditions [J]. Journal of Progress in Materials Science, 2014, 60: 130−207.

[16] DJAVANROODI F, EBRAHIMI M. Effect of die channel angle, friction and back pressure in the equal channel angular pressing using 3D finite element simulation [J]. Materials Science and Engineering A, 2010, 527: 1230−1235.

[17] EBRAHIMI M, DJAVANROODI F. Experimental and numerical analyses of pure copper during ECFE process as a novel severe plastic deformation method [J]. Progress in Natural Science: Materials International, 2014, 24: 68−74.

[18] EBRAHIMI M, PAR M A. Twenty-year uninterrupted endeavor of friction stir processing by focusing on copper and its alloys [J]. Journal of Alloys and Compounds, 2019, 781: 1074−1090.

[19] ABRAMOVA M M, ENIKEEV N, VAKIEV R Z, ETIENNE A, RADIGUET B, IVANISENKO Y, SAUVAGE X. Grain boundary segregation induced strengthening of an ultrafine-grained austenitic stainless steel [J]. Materials Letters, 2014, 136: 349−352.

[20] SHAARBAF M, TOROGHINEJAD M R. Nano-grained copper strip produced by accumulative roll bonding process [J]. Materials Science and Engineering A, 2008, 473: 28−33.

[21] EBRAHIMI M. Fatigue behaviors of materials processed by planar twist extrusion [J]. Metallurgical and Materials Transactions A, 2017, 48: 6126−6134.

[22] SAJADI A, EBRAHIMI M, DJAVANROODI F. Experimental and numerical investigation of Al properties fabricated by CGP process [J]. Materials Science and Engineering A, 2012, 552: 97−103.

[23] SATHEESH K S S, RAGHU T. Strain path effects on microstructural evolution and mechanical behaviour of constrained groove pressed aluminium sheets [J]. Materials and Design, 2015, 88: 799−809.

[24] KHODABAKHSHI F, ABBASZADEH M, ESKANDARI H, MOHEBPOUR S R. Application of CGP-cross route process for microstructure refinement and mechanical properties improvement in steel sheets [J]. Journal of Manufacturing Processes, 2013, 15: 1−9.

[25] MORADPOUR M, KHODABAKHSHI F, ESKANDARI H. Dynamic strain aging behavior of an ultra-fine grained Al−Mg alloy (AA5052) processed via classical constrained groove pressing [J]. Journal of Materials Research and Technology, 2019, 8: 630−643.

[26] JANDAGHI M R, POURALIAKBAR H. Study on the effect of post-annealing on the microstructural evolutions and mechanical properties of rolled CGPed aluminum−manganese−silicon alloy [J]. Materials Science and Engineering A, 2017, 679: 493−503.

[27] KHODABAKHSHI F, HAGHSHENAS M, ESKANDARI H, KOOHBOR B. Hardness−strength relationships in fine and ultra-fine grained metals processed through constrained groove pressing [J]. Materials Science and Engineering A, 2015, 636: 331−339.

[28] SATHEESH K S S, RAGHU T. Structural and mechanical behaviour of severe plastically deformed high purity aluminium sheets processed by constrained groove pressing technique [J]. Materials and Design, 2013, 57: 114−120.

[29] SARKARI KHORRAMI M, KAZEMINEZHAD M, KOKABI A H. Thermal stability during annealing of friction stir welded aluminum sheet produced by constrained groove pressing [J]. Materials and Design, 2013, 45: 222−227.

[30] EBRAHIMI M, ATTARILAR S, DJAVANROODI F, GODE C, KIM H S. Wear properties of brass samples subjected to constrained groove pressing process [J]. Materials and Design, 2014, 63: 531−537.

[31] DARMIANI E, DANAEE I, GOLOZAR M A, TOROGHINEJAD M R. Corrosion investigation of Al−SiC nano-composite fabricated by accumulative roll bonding (ARB) process [J]. Journal of Alloys and Compounds, 2013, 552: 31−39.

[32] NIE M Y, WANG C T, QU M H, GAO N, WHARTON J A, LANGDON T G. The corrosion behaviour of commercial purity titanium processed by high-pressure torsion [J]. Journal of Materials Science, 2014, 49: 2824−2831.

[33] NEJADSEYFI O, SHOKUHFAR A, DABIRI A, AZIMI A. Combining equal-channel angular pressing and heat treatment to obtain enhanced corrosion resistance in 6061 aluminum alloy [J]. Journal of Alloys and Compounds, 2015, 648: 912−918.

[34] ZHENG Z J, GAO Y, GUI Y, ZHU M. Corrosion behaviour of nanocrystalline 304 stainless steel prepared by equal channel angular pressing [J]. Corrosion Science, 2012, 54: 60−67.

[35] JIANG Jing-hua, MA Ai-bin, SONG Dan, YANG Dong-hui,

SHI Jun, WANG Kai-le, ZHANG Liu-yan, CHEN Jian-qing. Anticorrosion behavior of ultrafine-grained Al−26wt.%Si alloy fabricated by ECAP [J]. Journal of Materials Science, 2012, 47: 7744−7750.

[36] AKIYAMA E, ZHANG Z G, WATANABE Y, TSUZAKI K. Effects of severe plastic deformation on the corrosion behavior of aluminum alloys [J]. Journal of Solid State Electrochemistry, 2009, 13: 277−282.

[37] HOCKAUF M, MEYER L W, NICKEL D, ALISCH G, LAMPKE T, WIELAGE B, KRUGER L. Mechanical properties and corrosion behaviour of ultrafine-grained AA6082 produced by equal-channel angular pressing [J]. Journal of Materials Science, 2008, 43: 7409−7417.

[38] SONG D, MA A B, JIANG J H, LIN P H, YANG D H, FAN J F. Corrosion behavior of equal-channel-angular-pressed pure magnesium in NaCl aqueous solution [J]. Corrosion Science, 2010, 52: 481−490.

[39] JIANG J H, MA A B, SONG D, SAITO N, YUAN Y C, NISHIDA Y. Corrosion behavior of hypereutectic Al−23%Si alloy (AC9A) processed by severe plastic deformation [J]. Transactions of Nonferrous Metals Society of China, 2010, 20: 195−200.

[40] SONG D, MA A B, JIANG J H, LIN P H, YANG D H. Corrosion behavior of ultra-fine grained industrial pure Al fabricated by ECAP [J]. Transactions of Nonferrous Metals Society of China, 2009, 19: 1065−1070.

[41] PENG K P, ZHANG Y, SHAW L L, QIAN K W. Microstructure dependence of a Cu−38Zn alloy on processing conditions of constrained groove pressing [J]. Acta Materialia, 2009, 57: 5543−5553.

[42] MCCAFFERTY E. Validation of corrosion rates measured by the Tafel extrapolation method [J]. Corrosion Science, 2005, 47: 3202−3215.

[43] DJAVANROODI F, OMRANPOUR B, EBRAHIMI M, SEDIGHI M. Designing of ECAP parameters based on strain distribution uniformity [J]. Progress in Natural Science: Materials International, 2012, 22: 452−460.

[44] LEE H J, AHN B, KAWASAKI M, LANGDON T G. Evolution in hardness and microstructure of ZK60A magnesium alloy processed by high-pressure torsion [J]. Journal of Materials Research and Technology, 2015, 4: 18−25.

[45] KAWASAKI M, FIGUEIREDO R B, HUANG Y, LANGDON T G. Interpretation of hardness evolution in metals processed by high-pressure torsion [J]. Journal of Materials Science, 2014, 49: 6586−6596.

[46] WANG Y C, LANGDON T G. Effect of heat treatment on microstructure and microhardness evolution in a Ti−6Al−4V alloy processed by high-pressure torsion [J]. Journal of Materials Science, 2013, 48: 4646−4652.

[47] ANSARIAN I, SHAERI M H, EBRAHIMI M, MINARIK P, BARTHA K. Microstructure evolution and mechanical behaviour of severely deformed pure titanium through multi directional forging [J]. Journal of Alloys and Compounds, 2019, 776: 83−95.

[48] EBRAHIMI M, ATTARILAR S, SHAERI MH, GODE C, ARMOON H, DJAVANROODI F. An investigation into the effect of alloying elements on corrosion behavior of severely deformed Cu−Sn alloys by equal channel angular pressing [J]. Archives of Civil and Mechanical Engineering, 2019, 19: 842−850.

[49] DASHTI A, SHAERI M H, TAGHIABADI R, DJAVANROODI F, GHAZVINI F V, JAVADI H. Microstructure, texture, electrical and mechanical properties of AA-6063 processed by multi directional forging [J]. Materials, 2018, 11: 1−17.

[50] SHAERI M H, SALEHI M T, SEYYEDEIN S H, ABUTALEBI M R, PARK J K. Microstructure and mechanical properties of Al-7075 alloy processed by equal channel angular pressing combined with aging treatment [J]. Materials and Design, 2014, 57: 250−257.

[51] AMBAT R, DAVENPORT A J, SCAMANS G M, AFSETH A. Effect of iron-containing intermetallic particles on the corrosion behaviour of aluminium [J]. Corrosion Science, 2006, 48: 3455−3471.

[52] WU Y, LIAO H C. Corrosion behavior of extruded near eutectic Al−Si−Mg and 6063 alloys [J]. Journal of Materials Science and Technology, 2013, 29: 380−386.

[53] ECKERMANN F, SUTER T, UGGOWITZER P J, AFSETH A, SCHMUTZ P. The influence of MgSi particle reactivity and dissolution processes on corrosion in Al−Mg−Si alloys [J]. Electrochimica Acta, 2008, 54: 844−855.

[54] BUCHHEIT R G. A Compilation of corrosion potentials reported for intermetallic phases in aluminum alloys [J]. Journal of the Electrochemical Society, 1995, 142: 3994−3996.

[55] RALSTON K D, BIRBILIS N. Effect of grain size on corrosion: A review [J]. Corrosion, 2010, 66: 075005.

[56] SIKORA E, WEI X J, SHAW B A. Corrosion behavior of nanocrystalline bulk Al−Mg-based alloys [J]. Corrosion Science, 2004, 46: 387−398.

[57] KUS E, LEE Z, NUTT S, MANSFELD F. A comparison of the corrosion behavior of nanocrystalline and conventional Al 5083 samples [J]. Corrosion, 2006, 62: 152−161.

[58] CHUNG M K, CHOI Y S, KIM J G, KIM Y M, LEE J C. Effect of the number of ECAP pass time on the electrochemical properties of 1050 Al alloys [J]. Materials Science and Engineering A, 2004, 366: 282−291.

[59] SON I J, NAKANO H, OUE S, KOBAYASHI S, FUJUSHIMA H, HORITA Z. Pitting corrosion resistance of ultrafine-grained aluminum processed by severe plastic deformation [J]. Materials Transactions, 2005, 69: 892−898.

# 限制模压变形法提高 AA6063 铝合金的力学性能和耐腐蚀性

范仁杰[1], Shokouh ATTARILAR[2], Mahmoud SHAMSBORHAN[3,4],
Mahmoud EBRAHIMI[5], Ceren GÖDE[6], Hatice Varol ÖZKAVAK[7]

1. 铜陵职业技术学院 机械工程系，铜陵 244061;
2. School of Metallurgy and Materials Engineering, Iran University of Science and Technology, Tehran, Iran;
3. Department of Engineering, Mahabad Branch, Islamic Azad University, Mahabad, Iran;
4. Department of Mechanical Engineering, University of Zakho, Zakho, Kurdistan Region, Iraq;
5. Department of Mechanical Engineering, Faculty of Engineering, University of Maragheh, Maragheh, Iran;
6. School of Denizli Vocational Technology, Program of Machine, Pamukkale University, Denizli, Turkey;
7. Department of Mechanical and Metal Technology, Technical Sciences Vocational School,
Isparta University of Applied Sciences, Isparta, Turkey

**摘　要**：利用限制模压变形(CGP)法对 AA6063 铝合金进行塑性变形，改善其表面性能。结果发现，在第一道次后，合金的硬度值显著提高，硬度均匀性显著降低。而经后续的道次后，加工材料的硬度行为得到改善。此外，道次数增加后，在 CGP 第一道次中形成的细长晶粒逐渐转变为等轴晶粒。通过 CGP 工艺，样品的耐腐蚀性能提高，这是因为钝化膜的快速形成以及第二相和析出物形貌的变化阻碍它们的电化学反应，减少潜在的局部腐蚀位点。

**关键词**：力学性能；耐腐蚀性；铝合金；限制模压变形技术；晶粒细化；晶粒细化演变

**(Edited by Wei-ping CHEN)**